

# The Loss of the Chloride Channel, ClC-5, Delays Apical Iodide Efflux and Induces a Euthyroid Goiter in the Mouse Thyroid Gland

Marie-France van den Hove, Karine Croizet-Berger, François Jouret, Sandra E. Guggino, William B. Guggino, Olivier Devuyt, and Pierre J. Courtoy

Cell Biology Unit (M.-F.v.d.H., K.C.-B., P.J.C.), Christian de Duve Institute of Cellular Pathology, and Nephrology Unit (F.J., O.D.), Université catholique de Louvain, B-1200 Brussels, Belgium; and The Johns Hopkins University School of Medicine (S.E.G., W.B.G.), Baltimore, Maryland 21205

Genetic inactivation of ClC-5, a voltage-gated chloride channel prominently expressed in the kidney, leads to proteinuria because of defective apical endocytosis in proximal tubular cells. Because thyroid hormone secretion depends on apical endocytosis of thyroglobulin (Tg), we investigated whether ClC-5 is expressed in the thyroid and affects its function, using *Clcn5*-deficient knockout (KO) mice. We found that ClC-5 is highly expressed in wild-type mouse thyroid (~40% of mRNA kidney level). The protein was immunolocalized at the apical pole of thyrocytes. In Percoll gradients, ClC-5 overlapped with plasma membrane and early endosome markers, but best co-distributed with the late endosomal marker, Rab7. ClC-5 KO mice were euthyroid (normal T<sub>4</sub> and TSH serum levels) but developed a goiter with parallel iodine and Tg accumulation (*i.e.* normal Tg iodination level). When comparing ClC-5 KO

with wild-type mice, thyroid <sup>125</sup>I uptake after 1 h was doubled, incorporation into Tg was decreased by approximately 2-fold, so that trichloroacetic acid-soluble <sup>125</sup>I increased approximately 4-fold. Enhanced <sup>125</sup>I<sup>-</sup> efflux upon perchlorate and presence of <sup>125</sup>I-Tg as autoradiographic rings at follicle periphery demonstrated delayed iodide organification. Endocytic trafficking of <sup>125</sup>I-Tg toward lysosomes was not inhibited. Expression of pendrin, an I<sup>-</sup>/Cl<sup>-</sup> exchanger involved in apical iodide efflux, was selectively decreased by 60% in KO mice at mRNA and protein levels. Thus, ClC-5 is well expressed in the thyroid but is not critical for apical endocytosis, contrary to the kidney. Instead, the goiter associated with ClC-5 KO results from impaired rate of apical iodide efflux by down-regulation of pendrin expression. (*Endocrinology* 147: 1287–1296, 2006)

THE ClC CHLORIDE channels are voltage-gated channels involved in a broad range of physiological functions in mammals. The family includes nine isoforms, which operate at the plasma membrane or intracellular vesicles (1–3). The functional inactivation of several of these isoforms has been associated with diseases in man and mouse, pointing to a role in transepithelial transport, vesicular acidification, and endocytic trafficking (1, 3). ClC-5 is mainly expressed in the kidney, where it has been located in different tubular cell types, including the cells lining the proximal tubules, proximal tubular cells (PTC). Although ClC-5 has been localized in early endosomes in mouse kidney (4) and PTC in culture (5), it occurs at the cell surface when expressed in *Xenopus* oocytes or HEK 293 cells, where it mediates plasma membrane currents (6). ClC-5 elicits outward rectifying anion currents, with a selectivity for Br<sup>-</sup> greater than Cl<sup>-</sup> and Cl<sup>-</sup> greater than I<sup>-</sup> (1). Inactivating mutations of ClC-5 in patients with Dent's disease (X-linked familial nephrolithiasis), cause low-molecular-weight proteinuria and calciuria, which are reproduced in ClC-5 knockout (KO) mice

(1, 5, 7–9). The tubular proteinuria caused by the loss of ClC-5 results from defective receptor-mediated apical endocytosis of ultrafiltrated low-molecular weight proteins by kidney proximal tubules (4, 7), which reflects a trafficking defect of their multiligand receptors megalin and cubilin (10). It is currently proposed that ClC-5 may have a role in proper endosomal acidification, which is necessary to support normal vesicular trafficking, by providing the anion conductance linked to the electrogenic vacuolar H<sup>+</sup>-ATPase (1, 3, 11). Two independent studies (12, 13) have recently shown that the mammalian ClC-5 can also function as chloride/proton exchanger, similar to the *Escherichia coli* ClC-ec1 isoform (14), when activated by positive voltages. It may thus be regarded as an antiporter that could control endosomal acidification by coupling Cl<sup>-</sup> gradients to vesicular pH gradients.

A key step in thyroid hormone secretion is the apical endocytosis of the prohormone thyroglobulin (Tg). This is followed by their proteolytic release as a result of cathepsins in the late endocytic apparatus (15) and their secretion across the basolateral membrane. Moreover, the rate of thyroid hormone production correlates with the expression of endocytic catalysts promoting Tg uptake (Rab5) and transfer to late endosomes-lysosomes (Rab7), respectively (16). Being present at a huge concentration in the follicular lumen, Tg is predominantly internalized by fluid-phase endocytosis and addressed to lysosomes. In addition, selective receptor-mediated endocytosis has been reported at low Tg concentration

First Published Online November 23, 2005

Abbreviations: CFTR, Cystic fibrosis transmembrane conductance regulator; GAPDH, glyceraldehyde-3-phosphate dehydrogenase; KO, knockout; PB<sup>125</sup>I, protein-bound serum <sup>125</sup>I; PTC, proximal tubular cells; TCA, trichloroacetic acid; Tg, thyroglobulin; WT, wild type.

*Endocrinology* is published monthly by The Endocrine Society (<http://www.endo-society.org>), the foremost professional society serving the endocrine community.

*in vitro* (17, 18), but the identity of the receptor(s) involved remains elusive. The multiligand receptor megalin, which can interact with Tg, occurs at the apical surface of thyrocytes (19, 20), but its role in thyroid hormone secretion remains controversial. In most absorptive epithelial cells, including kidney PTC, megalin mediates transfer to lysosomes for degradation. In polarized rat FRTL-5 cells, megalin promotes Tg endocytosis, but the prohormone internalized by this mechanism was reported to bypass lysosomal degradation and be released in the basolateral medium by transcytosis (19, 21).

Active I<sup>-</sup> uptake by thyrocytes, transfer to the follicular lumen, and incorporation into Tg are key steps in thyroid hormone synthesis. In polarized thyrocyte monolayers, transepithelial traffic of I<sup>-</sup> is from basolateral to apical (22). Iodide is actively transported at the basolateral membrane by the Na<sup>+</sup>/I<sup>-</sup> symporter, NIS/SLC5A5 (23), and rapidly transferred to the follicular lumen by apical iodide channel(s) acutely regulated by TSH (21). The I<sup>-</sup>/Cl<sup>-</sup> apical exchanger pendrin (PDS/SLC26A4) is defective in Pendred's syndrome (24, 25) and is regarded as a key, but not exclusive, mediator of apical iodide efflux (25–28).

The presence of Cl<sup>-</sup> in the thyroid follicular lumen is necessary to support I<sup>-</sup> efflux by the pendrin exchanger (29). Cl<sup>-</sup> is vectorially transported through the basolateral (Na<sup>+</sup>K<sup>+</sup>2Cl<sup>-</sup>) symporter and apical anion channel(s), the molecular identity of which remains unknown (30). Electrophysiological studies have identified in the apical membrane of thyrocytes low-conductance Cl<sup>-</sup> currents regulated by cAMP (31, 32). The cystic fibrosis transmembrane conductance regulator (CFTR) controlled by phosphorylation via cAMP-dependent and other kinases, is the only apical Cl<sup>-</sup> channel demonstrated in the thyroid gland at mRNA and protein levels (33). Although the thyroid function is preserved in patients with cystic fibrosis under appropriate iodine supply, they are more susceptible to hypothyroidism upon iodide excess, suggesting that CFTR could participate in apical iodide efflux (34). No member of the CIC chloride channel family has so far been reported in the thyroid gland.

The present study aimed at investigating the expression of CIC-5 in the thyroid gland and its possible role in apical Tg endocytosis. We first showed that CIC-5 is abundantly expressed in the mouse thyroid. Second, to explore its function therein, we took advantage of CIC-5 KO mice. Our data show that CIC-5 is not critical for Tg endocytosis in the thyroid. Instead, CIC-5 inactivation leads to a euthyroid goiter with

delayed apical I<sup>-</sup> efflux, associated with a decrease of pendrin expression.

## Materials and Methods

### Animals

Two groups, each of 30 wild-type (WT) C57BL/6J male mice, 6 wk of age, were used for studies of CIC-5 expression and distribution in the thyroid. Three groups (A, B, and C) of CIC-5 KO male mice (*Cln5*<sup>-/-</sup>), created by deletion of exon VI of *Cln5* (7), were compared with WT (*Cln5*<sup>+/+</sup>) age-matched adult male mice. The effect of aging was further analyzed by comparing adult mice at 5 and 12 months of age (experiment B, in which a perchlorate discharge test was performed at 12 months). The thyroid of a male Wistar rat was used for deglycosylation experiments. Investigations were carried out in accordance with National Institutes of Health regulations for the care and use of laboratory animals.

### RNA extraction and mRNA measurement

Total RNA was isolated from pooled thyroids of 30 WT mice and from one kidney with the RiboPure kit followed by DNase I digestion (Ambion, Austin, TX). Total RNA was reverse transcribed into cDNA using ThermoScript RT-PCR System with total RNA primed with oligo(dT) (Invitrogen, Merelbeke, Belgium). RT-PCR were performed with 500 nmol/liter of both sense and antisense primers (Eurogentec, Seraing, Belgium; see sequence in Table 1) in a final volume of 20 μl (MyiQ; Bio-Rad, Hercules, CA). Size and purity of produced amplicons were analyzed by gel electrophoresis. Real-time PCR conditions were performed with denaturation at 95 C for 10 min, followed by 45 cycles of 20 sec at 95 C, 30 sec at 60 C, and 10 sec at 50 C. The melting temperature of PCR products was checked at the end of each PCR by recording SYBR green fluorescence decrease upon slowly denaturing DNA. Expression of CIC-5 in normal mouse thyroid was compared with that in kidney by semiquantitative RT-PCR and by real-time PCR, as reported (35). For relative mRNA quantification in WT and CIC-5 KO mice, real-time PCR analyses were performed in duplicate on total RNA extracted from single thyroid lobes of five different mice or on 400 ng total RNA of three kidneys. To normalize for differences in the amount of total RNA added to the reaction, mRNA levels of the target genes were adjusted to glyceraldehyde-3-phosphate dehydrogenase (GAPDH) mRNA levels determined simultaneously, after confirmation that this internal control was not affected by CIC-5 deletion. The reaction conditions were optimized to ensure that PCR efficiencies of the target genes and GAPDH gene were comparable, using standard curves of serial dilutions of normal mouse thyroid and kidney cDNA. Because mRNA levels of pendrin, megalin, Rab5a, and Rab7 in the kidney were not influenced by the loss of CIC-5, relative changes in mRNA level in thyroids of WT and KO mice were determined by comparison with kidney mRNA level using the 2<sup>-ΔΔCt</sup> method (35, 36). Results were expressed as normalized thyroid values relative to the kidney chosen as the calibrator.

**TABLE 1.** Primer sequences

Gene		Sequences (5'–3')	Amplicon size (bp)
CIC-5	Sense	AAGTGGACCCTTGTCATCAA	135
	Antisense	ACAAGATGTTCCCACAG (exon IV)	
Pendrin	Sense	GGAAAAGTCTACGCCACAA (1317–1337)	72
	Antisense	GCTTATCCCAAAGGCAATGA (1369–1389)	
Megalyn	Sense	CACAGGTGACTGTACCAGAA (13762–13781)	380
	Antisense	GTCAGTGTCTAAATGTTCCC (14141–14122)	
Rab5a	Sense	GACTTAGCAAATAAAAGAGC (874–894)	75
	Antisense	TCACTAAGGTCTACTCCTCG (1057–1077)	
Rab7	Sense	TCAATATGCGTCCCTCCTC (833–851)	73
	Antisense	TGGAGTTTCTTTTGGCAGC (887–905)	
GAPDH	Sense	TGCACCACCAACTGCTTAGC	176
	Antisense	GGATGCAGGGATGATGTTCT (exon I)	

### Analytical subcellular fractionation

Thyroid glands from 30 WT mice or from four pairs of WT and CIC-5 KO mice injected with <sup>125</sup>I at 1 h before euthanasia were pooled and homogenized in 250 mM sucrose, 10 mM Tris, pH 7.4. One kidney homogenate was prepared similarly for comparison. Thyroid homogenates were centrifuged at 134,000 × g for 45 min to isolate a high-speed pellet and a supernatant, in both of which total and trichloroacetic acid (TCA)-soluble radioactivity was measured when appropriate. The pellet was suspended in the initial volume of buffer, loaded onto 20% (vol/vol) Percoll (Amersham Pharmacia, Roosendaal, The Netherlands) in sucrose-Tris buffer and further resolved by centrifugation at 53,000 × g for 30 min (16, 37). Eleven fractions, collected from the bottom, were assayed for density and cathepsin D activity, and aliquots of equal volume were analyzed by Western blotting. Radioactivity was measured to compare <sup>125</sup>I trafficking in WT and KO mice.

### Western blotting

Homogenates, high-speed pellets, and fractions of the Percoll gradient were resolved by SDS-PAGE and transferred onto polyvinylidene fluoride membrane as previously described (16). After blocking, membranes were incubated overnight at 4°C with the following primary rabbit antibodies: CIC-5 (7) (SB499; 1:1000), megalin (a kind gift of Dr. P. J. Verroust, Hôpital St. Antoine, Paris, France; 1:10,000), Rab5a (Santa Cruz Biotechnology, Santa Cruz, CA; 1:500), Rab7 (a kind gift of Dr. M. Zerial, Max-Planck Institute, Dresden, Germany; 1:2000), and the iodide symporter NIS (a kind gift from Dr. P. Kopp, Northwestern University, Chicago, IL; 1:1000); with chicken antimouse pendrin (also from Dr. P. Kopp; 1:1000); or mouse monoclonal antibody against the 31-kDa E1 subunit of the vacuolar H<sup>+</sup>-ATPase (a kind gift of Dr. S. Gluck, Washington University, St. Louis, MO; 1:1000) and the α1-subunit of Na<sup>+</sup>/K<sup>+</sup>-ATPase (Upstate Biotechnology, Lake Placid, NY; 1:2000). Western blots were revealed by appropriate secondary antibodies for rabbit (BioSource, Camarillo, CA), chicken (Promega, Leiden, The Netherlands) or mouse IgG (Biosource), followed by enhanced chemiluminescence (Perkin-Elmer, Zaventem, Belgium) and quantification by using Scion (Frederick, MD) IMAGE 4.0.2 (10).

### Light microscopy

A thyroid lobe was dissected from several WT and KO mice, immediately fixed by 4% formaldehyde in PBS (pH 7.4) for 2 h, embedded in paraffin, and stained with hematoxylin-eosin. For CIC-5 immunoperoxidase, 6-μm sections were first incubated for 30 min with 0.3% H<sub>2</sub>O<sub>2</sub> to inactivate the endogenous thyroperoxidase. Antigen retrieval and immunolabeling were performed as described (35). For autoradiography, 4-μm sections were covered with Ilford L4 emulsion (Kodak, Zaventem, Belgium) and exposed for 3 wk, as previously reported (38).

### <sup>125</sup>I uptake

Mice were injected with 15 μCi <sup>125</sup>I (IMS 30; Amersham Bioscience), either ip (experiment B) or iv (experiment C) at 1 h before euthanasia. After exsanguination, thyroid glands were carefully dissected out and <sup>125</sup>I uptake was individually measured. For the perchlorate discharge test, 100 μl of 10 mM NaClO<sub>4</sub> were injected ip at 1 h after <sup>125</sup>I pulse to two pairs of 12-month-old WT and CIC-5 KO mice that were killed 1 h later. Radioactivity remaining in thyroid glands was compared with the <sup>125</sup>I uptake measured in glands from two other pairs of mice of the same age without the iodide chase. Protein-bound serum <sup>125</sup>I (PB<sup>125</sup>I) was determined after TCA precipitation.

### Analytical procedures

Protein and [<sup>127</sup>I]iodine concentration were measured in individual homogenates and fractions as reported (16). Tg concentration in the homogenates was calculated from the proportion of 19S and 27S Tg in the high-speed supernatant, after centrifugation on 5–20% sucrose gradients and analysis at 210 nm of the distribution profile, as reported (16, 37). Cathepsin D activity was determined as described (37). T<sub>4</sub> concentration was measured by RIA using a commercially available kit for

mouse serum (Beckman Coulter Co., Marseille, France). Serum TSH was determined by RIA using a kit for rat TSH (Amersham Bioscience).

### Statistical analyses

Biochemical values for WT mice are presented as means ± SD; for KO mice, single results were considered significant when out of confidence limits at 95% for WT means.

## Results

### *CIC-5 is well expressed in mouse thyroid gland and is located at the apical pole of thyrocytes*

Previous studies have disclosed that CIC-5 is predominantly expressed in the kidney, with much lower mRNA contents in brain, liver, lungs, and testes; the thyroid gland was not examined (1, 5, 7). We found by semiquantitative and quantitative real-time PCR that CIC-5 mRNA is significantly expressed in mouse thyroid gland, reaching approximately 40% of kidney level (Fig. 1A). By Western blotting, CIC-5 protein level in the thyroid gland was approximately 15% of kidney (Fig. 1B). The electrophoretic pattern differed between the two organs; in the thyroid gland, the major species was a broad band at M<sub>r</sub> approximately 90, with an additional weak band at M<sub>r</sub> approximately 80 (lanes 1 and 2). The latter isoform was predominantly expressed in the kidney (lanes 5 and 6). Both immunoreactive bands in the thyroid gland were abolished when using antibodies preadsorbed on the immunogenic peptide (lane 3) and were absent from CIC-5 KO thyroid glands (lane 4). Because CIC-5 is a glycoprotein, we addressed the difference in electrophoretic mobility between the thyroid and the kidney by a comparative deglycosylation study (35). Treatment with N-glycosidase F shifted the CIC-5 bands of both organs to the same single narrow band of indistinguishable mobility (M<sub>r</sub> approximately 70), indicating that CIC-5 bears more glycan chains in the thyroid than in the kidney (data not shown).

CIC-5 was next localized in mouse thyroid gland by immunohistochemistry. A strong staining was observed at the apical pole of normal thyrocytes (Fig. 1C, left). The pattern of staining was heterogeneous between follicles and between groups of cells in the same follicle. No staining was found when sections were incubated with preimmune antiserum or with the immune serum preadsorbed on the immunogenic peptide (data not shown). There was no staining in CIC-5 KO thyroid gland (Fig. 1C, right).

### *CIC-5 KO mice develop a euthyroid goiter*

All 5-month-old CIC-5 KO mice that were examined developed a goiter (Fig. 2, A and B). By histology, this goiter showed follicles of normal size surrounded by mostly cubic thyrocytes, as in WT thyroid glands, filled with a colloid evenly stained with hematoxylin-eosin (Fig. 2, C and D). Composition was analyzed in three thyroid homogenates of WT and KO mice (experiments A–C). Because WT values showed little variation, they were pooled as a common reference group, to which individual KO values were compared (Table 2).

Thyroid enlargement in individual groups of KO mice, as measured by total protein content, varied from 1.7- to 5-fold. Goiter development was paralleled by a comparable increase

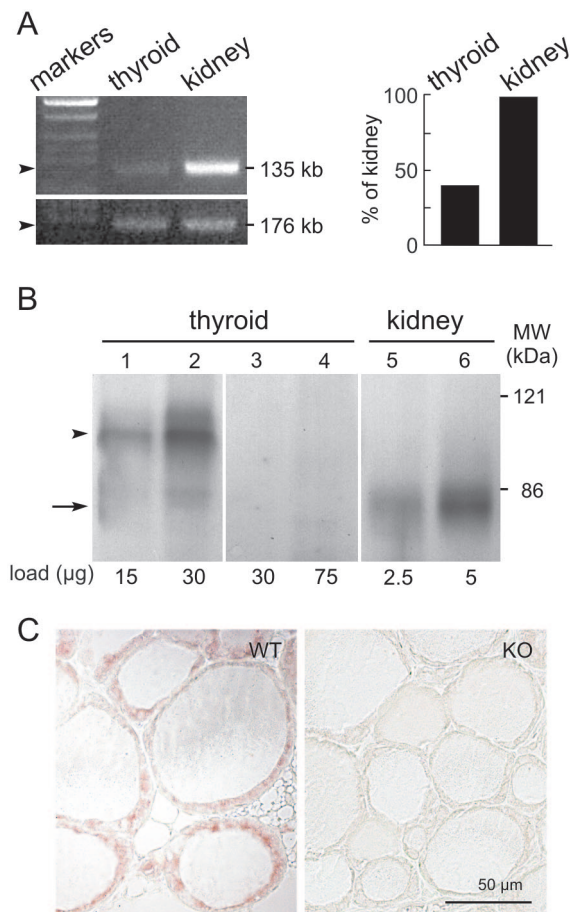


**FIG. 1.** The chloride channel, ClC-5, is well expressed in mice thyroid gland. **A**, RT-PCR. Expression of ClC-5 and GAPDH mRNA was compared in the thyroid gland and kidney by semiquantitative RT-PCR (left). ClC-5 mRNA was further measured by quantitative real-time PCR in duplicate, normalized to GAPDH mRNA, and expressed by reference to the kidney (100%; right). **B**, Western blotting. The protein amounts indicated below each lane for thyroid cells (*i.e.* total - Tg; lanes 1–4) and total kidney (lanes 5 and 6) were resolved by 7.5% SDS-PAGE and probed with the anti-ClC-5 rabbit antibodies. In the thyroid gland (lanes 1 and 2), ClC-5 mostly migrates as a broad band around  $M_r$  90 (arrowhead at left), and shows a minor band at  $M_r$  approximately 80 (arrow), its position in the kidney (lanes 5 and 6). Specific controls included antibody adsorption on immunogenic peptide (lane 3) and analysis of ClC-5 KO extracts (lane 4). **C**, Immunoperoxidase. In WT thyroid gland at left, ClC-5 is restricted to the apical cytoplasm of thyrocytes, with heterogeneous expression between cells. KO mice show no ClC-5 staining (right).

in soluble Tg. Sedimentation of soluble proteins on sucrose gradients revealed that a higher proportion of Tg occurred as 27S dimers in KO compared with WT mice ( $15 \pm 4$  vs.  $8 \pm 2\%$  of total Tg;  $n = 3$ ;  $P < 0.05$ ). Cellular protein, estimated as total protein minus Tg, also increased although less than Tg. Soluble thyroid iodine, which represented approximately 80–90% of total iodine in all groups of mice, showed higher increase than total and cellular proteins, from 2- to 8-fold. The ratio of total iodine to Tg, a *bona fide* reflection of Tg iodination level, was not different between WT and KO glands. Goiter and its biochemical parameters further increased with age in KO mice (Table 2, compare 5 vs. 12 months).

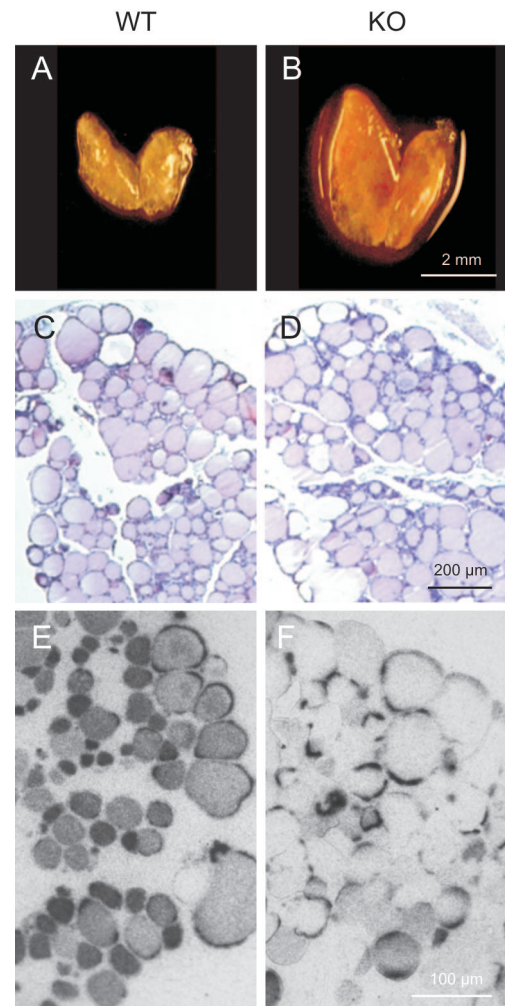


**FIG. 2.** Anatomy and functional histology: ClC-5 KO mice develop a goiter. **A** and **B**, Overview of the thyroid gland from 5-month-old WT and KO mice. Induction of goiter in the ClC-5 KO mice is obvious (see also Table 2). **C** and **D**, Conventional histology. There is no difference in mean follicle size between WT and KO mice, and colloid is homogeneously stained by hematoxylin-eosin. **E** and **F**, Autoradiography at 1 h after <sup>125</sup>I injection (part of experiment C, Table 2). In WT thyroid gland, most follicles show diffuse homogenous autoradiographic labeling of the colloid. In KO mice, labeling is predominantly restricted to a peripheral ring, indicating delayed mixing of [<sup>125</sup>I]Tg with the colloid.

#### *ClC-5 codistributes with endosomal and plasma membrane markers*

In kidney, ClC-5 colocalizes by immunofluorescence with the vacuolar H<sup>+</sup>-ATPase in subapical endosomes (11) and codistributes by analytical subcellular fractionation with vacuolar H<sup>+</sup>-ATPase (39) and the endosomal markers Rab5a and Rab7 (Auzanneau, C., R. Fuchs, G. Dom, S. E. Guggino, W. B. Guggino, O. Devuyt, and P. J. Courtoy, in preparation). We analyzed the thyroid subcellular distribution of ClC-5 in comparison with basolateral plasma membrane (NIS and Na<sup>+</sup>/K<sup>+</sup>-ATPase), apical plasma membrane (pendrin and megalin), and endosomal (vacuolar-ATPase and Rab5a for early endosomes; Rab7 for late endosomes) and lysosomal markers (cathepsin D activity). ClC-5-bearing particles distributed as a symmetrical peak in the light-density part of the

**TABLE 2.** Composition of thyroid glands in paired CIC-5 WT and KO mice

	WT		KO			
	Experiments A–C	Experiment B	Experiment A	Experiment B	Experiment C	Experiment B
Age (months)	5	12	5	5	5	12
Thyroid protein ( $\mu\text{g}/\text{gland}$ )						
Total	332 $\pm$ 26	711	509	719	1840	5304
Tg	177 $\pm$ 23	323	370	446	1086	3229
Cellular (total – Tg)	155 $\pm$ 21	388	139	273	754	2075
Soluble <sup>127</sup> I ( $\mu\text{g}/\text{gland}$ )	1.4 $\pm$ 0.2	3.8	3.7	4.9	9.7	26
Tg iodination level ( $\mu\text{g}$ iodine/100 $\mu\text{g}$ Tg)	0.8 $\pm$ 0.2	1.2	1.0	1.1	0.9	0.8

Homogenates of four thyroids were prepared from three groups (A, B, and C) of 5-month-old, or one group of 12-month-old (B) CIC-5 WT and KO mice. Results for WT mice were pooled and are means  $\pm$  SD ( $n = 3$ ). Results for KO mice were individual values considering the marked variability between groups. All values in CIC-5 KO mice are statistically different from WT ( $P < 0.05$ ), except for Tg iodination level.

Percoll gradient (Fig. 3B). CIC-5 was not resolved from the basolateral membrane marker Na<sup>+</sup>/K<sup>+</sup>-ATPase and the sodium/iodide symporter NIS (Fig. 3A). CIC-5 also largely overlapped with megalin (Fig. 3C). However, particles derived from the apical plasma membrane and bearing pendrin penetrated much more slowly in the gradient and were remarkably resolved from the distribution of megalin (Fig. 3C), indicating either that megalin in the thyroid gland is not abundant at the apical membrane but mostly occurs in endosomes (in the kidney proximal tubules, megalin occurs at both apical plasma membrane and endosomes) or that different apical domains were resolved. A denser shoulder of megalin distribution could indeed correspond to microvilli, as in kidney (10). CIC-5 also overlapped with vacuolar ATPase and with the early endosomal marker Rab5a (Fig. 3E)

and showed almost perfect codistribution with the late endosomal marker Rab7 (Fig. 3B). Finally, CIC-5 was fully resolved from lysosomes, the dense component of cathepsin D distribution (Fig. 3D). The cathepsin D activity that remained at the top of the gradient most likely reflects soluble enzymes released during homogenization.

#### CIC-5 KO mice show delayed iodide organification

The dynamics of iodide processing was further analyzed by following the fate of radioiodide at 1 h after injection, either ip or iv (Table 3). Iodide accumulation in the thyroid gland was 2- to 3-fold higher in CIC-5 KO than in WT mice. The thyroid content of <sup>125</sup>I remaining soluble in TCA increased even more (4- to 8-fold), whereas the fraction of total <sup>125</sup>I incorporated

**FIG. 3.** Subcellular fractionation: CIC-5 is resolved from pendrin and lysosomes and is not critical for Tg endocytosis and transport to lysosomes. A–E, Thyroid glands from 30 WT mice were pooled and homogenized, and a postnuclear supernatant was loaded on 20% Percoll (vol/vol, final). After centrifugation, 10 fractions were collected, analyzed for density (dotted line in B), cathepsin D activity (E), and Western blotting for the indicated constituents. The distribution of CIC-5 is superimposed in broken lines to other markers for comparison. F, Particulate pellets were isolated from homogenates of four thyroids obtained at 1 h after <sup>125</sup>I injection to 5-month-old WT and CIC-5 KO mice (experiment B) and run in parallel Percoll gradients to determine <sup>125</sup>I progression toward lysosomes. Radioactivity was TCA insoluble all over the gradient. Distributions are presented as percentage of the maximal value.

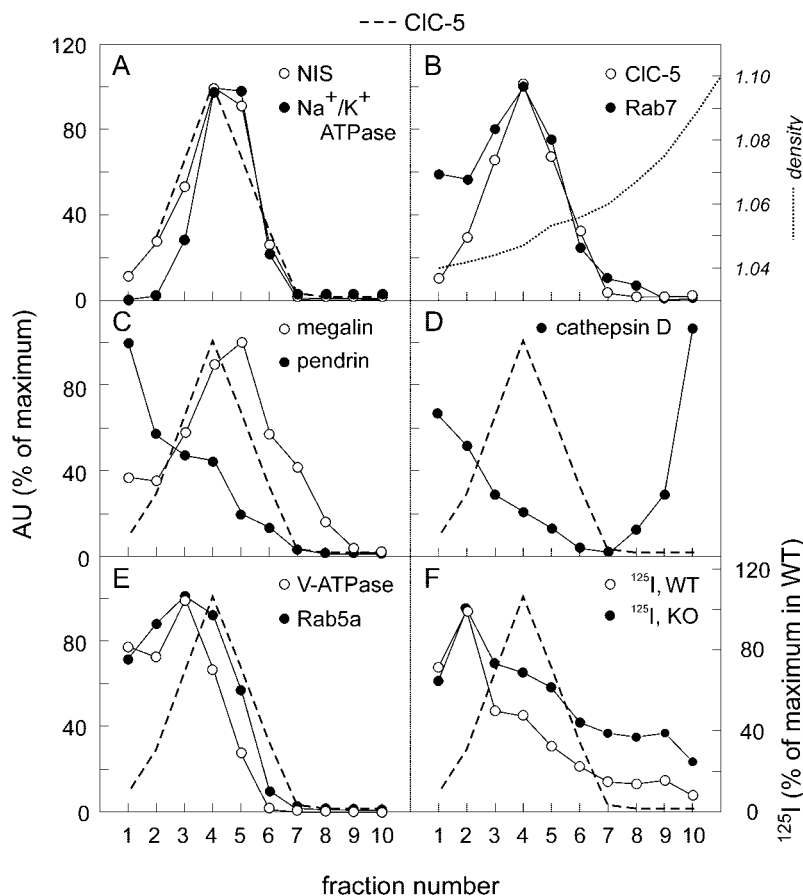


**TABLE 3.** Iodide processing in 5-month-old paired CIC-5 WT and KO mice

	WT	KO	KO/WT
Thyroid <sup>125</sup> I			
Uptake (%/h)			
B	0.27 ± 0.13 (6)	0.75 ± 0.17 <sup>a</sup> (5)	2.7
C	0.62 ± 0.13 (4)	1.13 ± 0.28 <sup>a</sup> (4)	1.8
<sup>125</sup> I in Tg (% of uptake)			
B–C	72–57	56–20	0.78–0.35
TCA-soluble [ <sup>125</sup> I]iodide (% of uptake)			
B–C	7–35	22–73	3.1–2.1
Serum			
PB <sup>125</sup> I (%/ml)			
B	9.5 ± 2.7 (5)	6.7 ± 1.4 (4)	0.7
C	13.8 ± 1.9 (4)	11.4 ± 2.2 (4)	0.8
T <sub>4</sub> (nM)	28.1 ± 4.6 (10)	29.5 ± 8.6 (8)	1.0
TSH (ng/ml)	3.3 ± 1.6 (5)	3.3 ± 0.9 (7)	1.0

<sup>125</sup>I was injected ip in mice of group B and iv in mice of group C (15 μCi/mouse). Pulse-labeling was for 1 h. Values are means ± SD (number of mice). Distribution of <sup>125</sup>I in Tg and of [<sup>125</sup>I]iodide soluble in TCA was measured in thyroid homogenates (see Table 2).

<sup>a</sup> *P* < 0.05.

into Tg was decreased in KO mice, pointing to a partial organification defect. This hypothesis was tested by a perchlorate discharge test performed in 12-month-old mice. In WT mice, 82% of the <sup>125</sup>I taken up in the thyroid at 1 h (0.33% of injected dose) remained in the gland after an additional 1 h of perchlorate chase, indicating that <sup>125</sup>I was rapidly organified. In contrast, the perchlorate discharge test was positive in KO mice; about 50% (55 and 38%) of <sup>125</sup>I taken up after 1 h (0.72% of injected dose) was free to exit from the gland upon the perchlorate chase, which strongly suggests a partial organification defect.

To characterize the process of organification at the tissue level, sections were analyzed by autoradiography at 1 h after <sup>125</sup>I injection. In WT thyroid glands, <sup>125</sup>I incorporation into Tg led to an even autoradiographic labeling of the colloid in most follicles, indicating no rate-limiting diffusion of radioiodine in the lumen and/or rapid mixing of newly iodinated Tg within the colloid (Fig. 2E). In contrast, in CIC-5 KO glands, the signal was weaker, pointing to poor retention of injected <sup>125</sup>I (because of defective incorporation in Tg). In addition, most follicles showed preferential retention of autoradiographic grains as peripheral rings, indicating a low mixing of newly labeled [<sup>125</sup>I]Tg with preexisting colloid (Fig. 2F). Taken together, these results suggested that CIC-5 deletion delayed iodide delivery to the extracellular site of organification.

#### *Tg trafficking and thyroid hormone secretion are not impaired in CIC-5 KO mice*

In kidneys, the loss of CIC-5 impairs receptor-mediated endocytosis by defective trafficking of megalin and cubilin (10). To assess whether similar changes occur in the thyroid, WT and CIC-5 KO mice were killed at 1 h after <sup>125</sup>I injection, thyroid glands were homogenized, and high-speed pellets were resolved by Percoll density gradients as above (Fig. 3F). In WT mice, one third of the <sup>125</sup>I remained at low density, compatible with association with plasma membrane particles marked by pendrin; half of the radioactivity was transferred to the endosomal region of the gradient (fractions 3–6), and only approximately 15% sedimented with lysosomes in the dense part of the gradient. In contrast, in KO mice, the proportion of <sup>125</sup>I reaching the density of the ly-

sosomal marker, cathepsin D, was doubled (~30%). These results indicate that, contrary to the kidney, endocytosis and transfer to lysosomes of newly iodinated [<sup>125</sup>I]Tg was not delayed but rather accelerated in CIC-5 KO mice.

Circulating levels of T<sub>4</sub> and TSH and of PB<sup>125</sup>I, an estimate of [<sup>125</sup>I]hormone secretion, were nearly identical in WT and CIC-5 KO mice (Table 3), indicating that KO mice are euthyroid. Altogether, these results show that CIC-5 absence in the thyroid gland does not slow down Tg endocytosis and proteolytic release of thyroid hormones and suggest that comparable PB<sup>125</sup>I levels in KO and in WT mice reflect the combination of accelerated endocytosis of newly iodinated Tg with fewer [<sup>125</sup>I]iodothyronine residues per Tg molecule.

#### *Pendrin expression is selectively decreased in CIC-5 KO mice*

The association of a euthyroid goiter with delayed iodide organification and positive perchlorate discharge test, as reported here, is highly reminiscent of patients with Pendred's syndrome (28). Therefore, we looked for the effect of CIC-5 deletion on pendrin expression by real-time PCR and Western blotting (Fig. 4). In CIC-5 KO mice, pendrin mRNA and protein levels were decreased by more than 60% in the thyroid glands compared with WT mice, with no difference in corresponding kidneys, indicating that the deficit of expression is specific for the thyroid gland. The decrease in pendrin mRNA expression in CIC-5 KO thyroid contrasted with normal thyroid and kidney mRNA levels for the apical membrane receptor megalin and for the two endocytic catalysts Rab5a and Rab7. Interestingly, comparison of mRNA levels between both organs of WT mice showed that pendrin expression in the thyroid reached only approximately 2% of the kidney level. Thyroid expression of megalin was also much lower (~5%) than in kidneys, but Rab5a and Rab7 mRNA levels were higher in the thyroid than in kidneys (780 and 150%, respectively). By Western blotting, megalin abundance was preserved or increased in the thyroid gland of CIC-5 KO mice, whereas that of the endocytic catalysts Rab5a and Rab7 was not altered (Fig. 4). The expression of the basolateral iodide symporter NIS (data not shown), which is not ex-

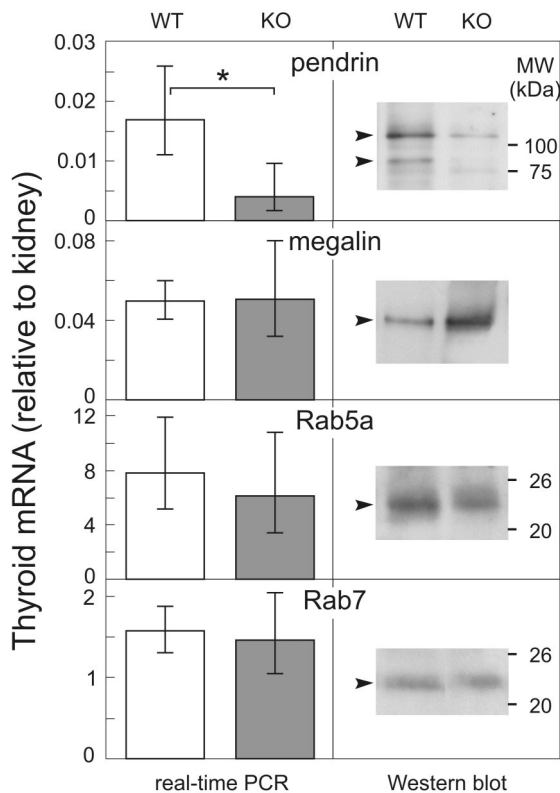


**FIG. 4.** Pendrin expression is selectively decreased in CIC-5 KO mice. *Left*, Real-time PCR. Expression in thyroid gland relative to kidney of pendrin, megalin, Rab5a, and Rab7 is compared in CIC-5 WT (white bars) and KO mice (gray bars). RNA was extracted individually from three kidney homogenates and five thyroid lobes. Because total RNA could not be measured in thyroid extracts, each mRNA level was adjusted to that of GAPDH. Data in thyroid, normalized to this endogenous reference, were then expressed relative to the same normalized value in kidney, taken as the unit. Kidney was arbitrarily chosen as the calibrator because no difference in pendrin, megalin, Rab5a, and Rab7 expression was found between kidneys of WT and CIC-5 KO mice. Results are means  $\pm$  SD. The asymmetric distribution of values is a consequence of converting the results of an exponential process (Ct is exponentially related to copy number) into a linear comparison of amounts (36). The only significant difference in CIC-5 KO mice is an approximately 4-fold decreased expression of pendrin mRNA in the thyroid ( $P < 0.05$ ). In WT mice, mRNA expression in the thyroid gland compared with the kidney is much lower for pendrin (1.8%) and megalin (5%), higher for Rab7 (150%), and much higher for Rab5a (780%). *Right*, Representative immunoblots of thyroid high-speed pellets from WT and CIC-5 KO mice (10  $\mu$ g protein per lane). Position of molecular mass markers is indicated at *right*. By densitometry, pendrin level in thyroid glands of KO mice was 40% of the WT level, megalin abundance was increased, and Rab5a and Rab7 were unchanged.

pressed in the kidney, was increased in the same proportion as the <sup>125</sup>I uptake.

### Discussion

This study shows that the chloride channel CIC-5 is abundantly expressed in mouse thyrocytes and that deletion of CIC-5 in mouse leads to a euthyroid goiter. The goiter is not caused primarily by Tg accumulation resulting from a deficit of endocytic uptake but results from the compensation by hyperplasia of delayed iodide organification, which correlates with a strong reduction of pendrin expression. Thus,

absence of CIC-5 in mice thyroid gland mimics the thyroidal phenotype of patients with Pendred's syndrome. These data offer new perspectives into the molecular mechanism of Tg endocytosis and on the role of CIC-5 in the thyroid.

*The loss of CIC-5 does not impair endocytic uptake of Tg and transfer to lysosomes: implications for the mechanisms of Tg endocytosis and trafficking*

The molecular mechanisms of apical Tg uptake, in particular the significance of a possible receptor-mediated endocytosis at the huge Tg luminal concentration ( $\sim 10$  g/100 ml), and the role of receptor(s) in intracellular trafficking to late endosomes/lysosomes where Tg proteolysis releases thyroid hormones are still debated. Tg is a ligand of megalin, a high-capacity receptor expressed at the apical membrane of thyrocytes (20). Competition by the receptor-associated protein has been presented as functional evidence for a role of megalin in receptor-mediated endocytosis of Tg by rat FRTL-5 cells *in vitro* (19, 21). Furthermore, intriguing observations were reported to suggest that megalin shows preference for Tg bearing low hormonogenic content and directs its intracellular trafficking to avoid lysosomes and to be released instead intact by transcytosis at the basolateral membrane. In contrast, hormone-rich Tg would be taken up by fluid-phase endocytosis and be transported to lysosomes for effective hormone release (20). However, no clear evidence has yet been provided for competition by receptor-associated protein in the uptake by thyrocytes of Tg at the huge concentration prevailing in the follicular lumen.

In kidney PTC, the loss of CIC-5 is associated with a major decrease (by  $\sim 7$ -fold) in receptor-mediated endocytosis of low-molecular-weight proteins. This endocytic defect is caused by a megalin trafficking defect, causing disappearance of the receptor from the apical plasma membrane where the protein cargo is taken up, associated with an additional impairment in cargo transfer to lysosomes (10). By contrast, we found no evidence for a deficit of megalin-mediated Tg endocytosis in the thyroid of CIC-5 KO mice. Indeed, the endocytic processing of hormone-rich [<sup>125</sup>I]Tg generated normal circulating T<sub>4</sub> levels. Moreover, uptake and transfer to lysosomes of pulse-labeled Tg at 1 h after <sup>125</sup>I injection were accelerated. Preferential endocytosis of [<sup>125</sup>I]Tg, present as autoradiographic rings at the periphery of the follicular lumen, is in agreement with the last-come, first-served model of Tg handling (40).

The contrast between accelerated transfer of [<sup>125</sup>I]Tg to lysosomes and normal release of <sup>125</sup>I-labeled thyroid hormones (measured as [<sup>125</sup>I]PBI) could be explained by delayed intramolecular coupling of [<sup>125</sup>I]iodotyrosyl side chains to generate [<sup>125</sup>I]thyronines in Tg (a mechanism highly dependent on the availability of iodine). An alternative explanation would be impairment of [<sup>125</sup>I]Tg proteolysis to release thyroid hormones in the late endocytic structures with which CIC-5 preferentially associates in the thyroid gland, for example by defective acidification (41). However, accelerated transfer of [<sup>125</sup>I]Tg to lysosomes and normal circulating T<sub>4</sub> levels in CIC-5 KO mice argue against a necessary role of CIC-5 in the acidification of the endosomal/lysosomal compartment where thyroid hormones are released from Tg.

Fluid-phase endocytosis is an alternative mechanism for uptake of Tg. In contrast to receptor-mediated endocytosis, fluid-phase endocytosis is not impaired in kidney PTC of CIC-5 KO mice (10). Thus, if Tg is essentially internalized into thyrocytes by this bulky mechanism as a consequence of its huge concentration found in the follicular lumen, a normal rate of Tg endocytosis in the thyroid gland of CIC-5 KO mice is to be expected. In fact, global release of thyroid hormones from Tg was preserved in CIC-5 KO mice, as shown by their euthyroid status, and thyroid expression of the rate-limiting endocytic catalysts Rab5a and Rab7 (16) was not changed, as in kidney (10). Moreover, we did not observe in the glands such large follicles surrounded by flat epithelial cells as occurring in aging mice when the rate of endocytosis is slowed down (42).

*The loss of CIC-5 is associated with a delay in iodide organification: implications for apical iodide transport*

Despite avid iodide thyroid uptake and parallel increase of the iodide symporter NIS abundance, the efficiency of <sup>125</sup>I incorporation into Tg was strongly decreased in CIC-5 KO mice, and diffusion of [<sup>125</sup>I]Tg in the colloid was far from being completed at 1 h after pulse. However, the normal <sup>127</sup>I iodination level of Tg indicates that the thyroperoxidase machinery for oxidation was qualitatively preserved. The accumulation of <sup>125</sup>I in a perchlorate-sensitive pool is thus consistent with a defect in its rate of apical efflux. The occurrence of a selective I<sup>-</sup> channel, impermeable to chloride and distinct from the CFTR, has been demonstrated by functional reconstitution into liposomes (43). However, the identity of this apical iodide channel is still unknown. A protein homologous to NIS but located at the apical membrane of

thyrocytes (SLC5A8) was initially proposed as a putative apical iodide transporter (44) but has since been identified as a transporter of short-chain fatty acids (45).

Recent functional studies in polarized MDCK cells expressing NIS have demonstrated that coexpression with WT pendrin, an I<sup>-</sup>/Cl<sup>-</sup> exchanger, is sufficient to mediate apical iodide transport. In contrast, coexpression of NIS with two PDS mutants, identified in a euthyroid patient having Pendred's syndrome, completely failed to promote iodide efflux, despite the only partial organification defect observed in this patient (27). This indicates that iodide may reach the follicular lumen independently of pendrin, as also indirectly supported by the clinically and biochemical euthyroid status of most individuals with Pendred's syndrome, at least under adequate nutritional iodide supply (24, 28), and by absence of a thyroidal phenotype in pendrin KO mice (46). The intrinsic partial transport deficit is thus fully compensated by an increased number of less active cells, which explains the euthyroid goiter of Pendred's patients. Different factors may account for the phenotypic variability of this adaptation mechanism in CIC-5 KO mice. First, nutritional iodide intake, known to be lower in Europe than in the United States, may become inadequate, leading to transient iodine deficiency with increased serum TSH level, especially at a crucial stage of development. Second, iodine turnover is much faster in mouse than in human. Indeed, daily thyroid T<sub>4</sub> secretion requires endocytosis of more than 25% of the iodine pool stored in Tg in the mouse but only 1% in the human. This might explain why Dent's patients do not apparently develop a goiter (Devuyst, O., and R. V. Thakker, unpublished data).

We therefore suggest that CIC-5 could act as an alternative

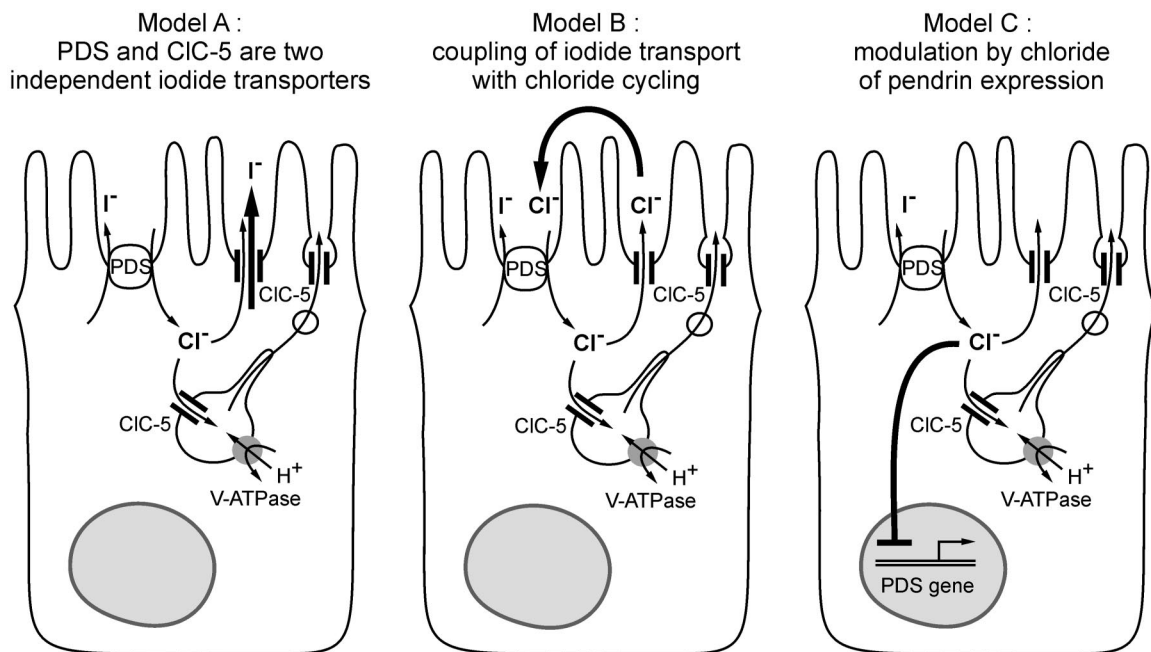


FIG. 5. Three models of CIC-5 channel function and interaction with pendrin (PDS) in normal thyrocytes. A, CIC-5 channel is an apical iodide channel. Despite Cl<sup>-</sup> preference over I<sup>-</sup>, CIC-5 channel supports apical efflux of I<sup>-</sup> from the thyroid cytoplasm, where it reaches much higher concentrations than in other cell types. B, CIC-5 channel supports chloride cycling necessary for the activity of pendrin, acting as an apical I<sup>-</sup>/Cl<sup>-</sup> exchanger in the thyrocyte. C, CIC-5 channel indirectly regulates pendrin expression.

iodide conductance at the apical plasma membrane (Fig. 5, model A). The occurrence of ClC-5 at the plasma membrane has been reported in other systems (1, 6) and is compatible with its overlapping density distribution with that of megalin. The thyrocyte cytosol contains 4 mM Cl<sup>-</sup>, and I<sup>-</sup> concentration can be much higher than in other cells. Usually low in physiological conditions (0.05–0.1 mM), free iodide can accumulate up to 2 mM in case of organification defect (26). Therefore, despite preference for other anions, ClC-5 could operate as an I<sup>-</sup> channel in thyrocytes. Although this possibility does not seem consistent with the chloride impermeability reported for the major functional iodide channel in liposomes (43), it might account for the alternative, less specific anionic conductance found in thyroid plasma membrane vesicles (47).

As a second possibility (Fig. 5, model B), ClC-5 might be necessary at the apical membrane of thyrocytes for recycling chloride to the follicular lumen, to support pendrin-mediated I<sup>-</sup>/Cl<sup>-</sup> antiport (29). At variance with the urine, Cl<sup>-</sup> concentration in the tightly closed follicular lumen is expected to be low in the absence of an apical Cl<sup>-</sup> conductance. In model B, ClC-5 may be crucial to replenish the luminal chloride pool.

A third possibility is that ClC-5 would act indirectly, by modulating pendrin expression in thyrocytes (Fig. 5, model C). The mechanism for the observed decrease in pendrin expression in ClC-5 KO thyroid glands and, conversely, the role of ClC-5 to maintain pendrin expression in normal thyrocytes but not in kidneys remains speculative. So far, a decrease in pendrin mRNA has been reported only in dedifferentiated thyroid carcinomas (48–50), whereas thyroid glands are well differentiated in ClC-5 KO mice. In kidneys, pendrin has been identified as a Cl<sup>-</sup>/HCO<sub>3</sub><sup>-</sup> exchanger regulated in response to chronic alterations in chloride balance. In particular, its expression was found to be reduced in response to metabolic acidosis, even before the decline in the number of pendrin-positive cells (51–53), and inversely related with diet-induced changes in chloride excretion (54). Because chloride concentration is much lower in the colloid than in urine, pendrin regulation might be more sensitive to any perturbation of chloride transport in thyrocytes than in kidney cells.

In conclusion, ClC-5 is abundantly expressed in the mouse thyroid gland but is not critical for apical endocytosis, contrary to kidney PTC. Instead, ClC-5 modulates the rate of apical iodide efflux, either by acting as an alternative iodide channel or by regulating pendrin expression and/or function. Our data suggest that ClC-5 may be important for Cl<sup>-</sup> homeostasis in the thyroid gland and is indeed needed for full operation of an apical anion transport specific to thyrocytes. Additional studies using transfection of polarized cells could allow resolving the precise mechanism of this new ClC-5 function.

### Acknowledgments

The superb technical assistance of M. Eppe, H. Debaix, and F. N'Kuli as well as the graphic and editorial assistance of M. Leruth and Y. Marchand are gratefully acknowledged. We thank J. Sipes for her assistance in the animal care. We express our gratitude to Drs. M. Zerial,

P. J. Verroust, P. Kopp, and S. Gluck for the kind gift of anti-Rab7, -megalin, -NIS and -pendrin, and -E1 v-ATPase antibodies, respectively.

Received September 7, 2005. Accepted November 11, 2005.

Address all correspondence and requests for reprints to: M.-F. van den Hove, M.D., Cell Unit-ICP/UCL 7541, 75 av Hippocrate, B-1200 Brussels, Belgium. E-mail: vandenhove@cell.ucl.ac.be.

This work was supported by Fonds National de la Recherche Scientifique, Forton, Actions de Recherche Concertées, and Interuniversity Attraction Poles of the Prime Minister's Services (Belgium), National Institutes of Health no. R24 64388 and European Union no. 005085. M.-F.v.d.H. is Research Associate of the National Fund for Scientific Research.

All authors have nothing to declare.

### References

- Jentsch TJ, Stein V, Weinreich F, Zdebik AA 2002 Molecular structure and physiological function of chloride channels. *Physiol Rev* 82:503–568
- Dutzler A, Campbell EB, Cadene M, Chait BT, MacKinnon R 2002 X-ray structure of a ClC chloride channel at 3.0 Å reveals the molecular basis of anion selectivity. *Nature* 415:287–294
- Devuyst O, Guggino W 2002 Chloride channels in the kidney: lessons from knockout animals. *Am J Physiol Renal Physiol* 283:1176–1191
- Piwon N, Günther W, Schwake M, Bösl MR, Jentsch TJ 2000 ClC-5 Cl-channel disruption impairs endocytosis in a mouse model for Dent's disease. *Nature* 408:369–373
- Devuyst O, Christie PT, Courtoy PJ, Beauwens R, Takker RV 1999 Intra-renal and subcellular distribution of the human chloride channel, ClC-5, reveals a pathophysiological basis for Dent's disease. *Hum Mol Genet* 8:247–257
- Friedrich T, Breiderhoff T, Jentsch TJ 1999 Mutational analysis demonstrates that ClC-4 and ClC-5 directly mediate plasma membrane currents. *J Biol Chem* 274:896–902
- Wang SS, Devuyst O, Courtoy PJ, Wang XT, Wang H, Wang Y, Thakker RV, Guggino S, Guggino WB 2000 Mice lacking renal chloride channel, ClC-5, are a model for Dent's disease, a nephrolithiasis disorder associated with defective receptor-mediated endocytosis. *Hum Mol Genet* 9:2937–2945
- Scheinman SS, Guay-Woodford LM, Thakker RV, Waronck DG 1999 Genetic disorders of renal electrolyte transport. *N Engl J Med* 340:1177–1187
- Günther W, Piwon N, Jentsch TJ 2003 The ClC-5 chloride channel knock-out mouse: an animal model for Dent's disease. *Pflügers Arch Eur J Physiol* 445:456–462
- Christensen EI, Devuyst O, Dom G, Nielsen R, Van Der Smissen P, Verroust P, Leruth M, Guggino WB, Courtoy PJ 2003 Loss of chloride channel ClC-5 impairs endocytosis by defective trafficking of megalin and cubilin in kidney proximal tubules. *Proc Natl Acad Sci USA* 100:8472–8477
- Günther W, Lüchow A, Cluzeaud F, Vandewalle A, Jentsch TJ 1998 ClC-5, the chloride channel mutated in Dent's disease, colocalizes with the proton pump in endocytically active kidney cells. *Proc Natl Acad Sci USA* 95:8075–8080
- Piccolo A, Pusch M 2005 Chloride/proton antiporter activity of mammalian ClC proteins ClC-4 and ClC-5. *Nature* 436:420–423
- Scheel O, Zdebik AA, Lourdel S, Jentsch TJ 2005 Voltage-dependent electrogenic chloride/proton exchange by endosomal ClC proteins. *Nature* 436:424–427
- Accardi A, Miller C 2004 Secondary active transport mediated by a prokaryotic homolog of ClC Cl<sup>-</sup> channels. *Nature* 427:803–807
- Dunn AD, Myers HE, Dunn JT 1996 The combined action of two thyroidal proteases releases T<sub>4</sub> from the dominant hormone-forming site of thyroglobulin. *Endocrinology* 137:3279–3285
- Croizat-Berger K, Daumerie C, Couvreur M, Courtoy PJ, van den Hove MF 2002 The endocytic catalysts, Rab5a and Rab7, are tandem regulators of thyroid hormone production. *Proc Natl Acad Sci USA* 99:8277–8282
- van den Hove MF, Couvreur M, De Visscher M, Salvatore G 1982 A new mechanism for the reabsorption of thyroid iodoproteins: selective fluid pinocytosis. *Eur J Biochem* 122:415–422
- Lemansky P, Herzog V 1992 Endocytosis of thyroglobulin is not mediated by mannose-6-phosphate receptors in thyrocytes: evidence for low-affinity-binding sites in the uptake of thyroglobulin. *Eur J Biochem* 209:111–119
- Marino M, Zheng G, McCluskey RT 1999 Megalin (gp330) is an endocytic receptor for thyroglobulin on cultured Fisher rat thyroid cells. *J Biol Chem* 274:12898–12904
- Lisi S, Pinchera A, McCluskey RT, Willnow TE, Refetoff S, Marcocci C, Vitti P, Menconi F, Grasso L, Luchetti F, Collins AB, Marino M 2003 Preferential megalin-mediated transcytosis of low-hormonogenic thyroglobulin: a control mechanism for thyroid hormone release. *Proc Natl Acad Sci USA* 100:14858–14863
- Marino M, Zheng G, Chiovato L, Pinchera A, Brown D, Andrews D, McCluskey RT 2000 Role of megalin (gp330) in transcytosis of thyroglobulin by

- thyroid cells: a novel function in the control of thyroid hormone release. *J Biol Chem* 275:7125–7137
22. Nilsson M, Björkman U, Ekholm R, Ericson LE 1990 Iodide transport in primary cultured thyroid follicle cells: evidence of a TSH-regulated channel mediating iodide efflux selectively across the apical domain of the plasma. *Eur J Cell Biol* 52:270–281
  23. De la Vieja A, Dohan O, Levy O, Carrasco N 2000 Molecular analysis of the sodium/iodide symporter: impact on thyroid and extrathyroid pathophysiology. *Physiol Rev* 80:1083–1105
  24. Scott DA, Wang R, Kreman T M, Sheffield V C, Karnishki LP 1999 The pendred syndrome gene encodes a chloride-iodide transport protein. *Nat Genet* 21:440–443
  25. Royaux IE, Suzuki K, Mori A, Katoh R, Everett LA, Kohn LD, Green ED 2000 Pendrin, the protein encoded by the Pendred syndrome gene (PDS), is an apical porter of iodide in the thyroid and is regulated by thyroglobulin in FRTL-5 cells. *Endocrinology* 141:839–845
  26. Yoshida A, Taniguchi S, Hisatome I, Royaux IE, Green ED, Kohn LD, Suzuki K 2002 Pendrin is an iodide-specific apical porter responsible for iodide efflux from thyroid cells. *J Clin Endocrinol Metab* 87:3356–3361
  27. Gillam MP, Sidhaye AR, Lee EJ, Rutishauser J, Waeber-Stephan C, Kopp P 2004 Functional characterization of pendrin in a polarized cell system: evidence for pendrin-mediated apical iodide efflux. *J Biol Chem* 279:13004–13010
  28. Kopp P 1999 Pendred's syndrome: clinical characteristics and molecular basis. *Curr Opin Endocrinol Diabetes* 6:261–269
  29. Yoshida A, Hisatome I, Taniguchi S, Sasaki N, Yamamoto Y, Miake J, Fukui H, Shimizu H, Okamura T, Okura T, Igawa O, Shigemasa C, Green ED, Kohn LD, Suzuki K 2004 Mechanism of iodide/chloride exchange by pendrin. *Endocrinology* 145:4301–4308
  30. Nilsson M 2001 Iodide handling by the thyroid epithelial cell. *Exp Clin Endocrinol Diabetes* 109:13–17
  31. Champigny G, Verrier B, Gérard C, Mauchamp J, Lazdunski M 1990 Small conductance chloride channels in the apical membrane of thyroid cells. *FEBS Lett* 259:263–268
  32. Bourke JR, Sand O, Abel KC, Huxham GJ, Manley SW 1995 Chloride channels in the apical membrane of thyroid epithelial cells are regulated by cyclic AMP. *J Endocrinol* 147:441–448
  33. Devuyst O, Golstein PE, Sanches MV, Piontek K, Wilson PD, Guggino WB, Dumont JE, Beauwens R 1997 Expression of CFTR in human and bovine thyroid epithelium. *Am J Physiol* 272:299–308
  34. Segall-Blank M, Vagenakis AG, Shwachman H, Ingbar SH, Braverman LE 1981 Thyroid gland function and pituitary reserve in patients with cystic fibrosis. *J Pediatr* 98:218–222
  35. Jouret F, Igarashi T, Gofflot F, Wilson PD, Karet FE, Thakker RV, Devuyst O 2004 Comparative ontogeny, processing, and segmental distribution of the renal chloride channel, ClC-5. *Kidney Int* 65:198–208
  36. Livak KJ, Schmittgen TD 2001 Analysis of relative gene expression data using real time quantitative PCR and the 2<sup>-ΔΔC<sub>T</sub></sup> method. *Methods* 25:402–408
  37. van den Hove MF, Couvreur M, Col V, Gervy C, Authélet M, Nève P 1995 T<sub>4</sub> accumulation in lysosomes of rat thyroid remnants after subtotal thyroidectomy. *Eur J Cell Biol* 68:437–445
  38. Gérard AC, Deneff JF, Colin IM, van den Hove MF 2004 Evidence for processing of compact insoluble thyroglobulin globules in relation with follicular cell functional activity in the human and the mouse thyroid. *Eur J Endocrinol* 150:73–80
  39. Moulin P, Igarashi T, Van Der Smissen P, Cosyns JP, Verroust P, Thakker RV, Scheinman SJ, Courtoy PJ, Devuyst O 2003 Altered polarity and expression of H<sup>+</sup>-ATPase without ultrastructural changes in kidneys of Dent's disease patients. *Kidney Int* 63:1285–1295
  40. Studer H, Gerber H 1991 Intrathyroidal iodine: heterogeneity of iodocompounds and kinetic compartmentalization. *Trends Endocrinol Metab* 2:29–34
  41. Hara-Chikuma M, Wang Y, Guggino SE, Guggino WB, Verkman AS 2005 Impaired acidification in early endosomes of ClC-5 deficient proximal tubule. *Biochem Biophys Res Commun* 329:941–946
  42. Gerber H, Peter HJ, Studer H 1987 Age related failure of endocytosis may be the pathogenic mechanism responsible for "cold" follicle formation in the aging mouse thyroid. *Endocrinology* 120:1758–1764
  43. Golstein PE, Sener A, Beauwens R 1995 The iodide channel of the thyroid. II. Selective iodide conductance inserted into liposomes. *Am J Physiol* 268:C111–C118
  44. Rodriguez AM, Perron B, Lacroix L, Caillou B, Leblanc G, Schlumberger M, Bidart JM, Pourchier T 2002 Identification and characterization of a putative human iodide transporter located at the apical membrane of thyrocytes. *J Clin Endocrinol Metab* 87:3500–3503
  45. Ganapathy V, Gopal E, Miyauchi S, Prasad PD 2005 Biological functions of SLC5A8, a candidate tumour suppressor. *Biochem Soc Trans* 33:237–240
  46. Everett LA, Belyantseva IA, Noben-Trauth K, Cantos R, Chen A, Thakkar SI, Hoogstraten-Miller SL, Kachar B, Wu DK, Green ED 2001 Targetted disruption of mouse *Pds* provides insight about the inner-ear defects encountered in Pendred syndrome. *Hum Mol Genet* 10:153–161
  47. Golstein P, Abramow M, Dumont JE, Beauwens R 1992 The iodide channel of the thyroid: a plasma membrane vesicle study. *Am J Physiol* 263C:590–597
  48. Bidart JM, Mian C, Lazar V, Russo D, Filetti S, Caillou B, Schlumberger M 2000 Expression of pendrin and Pendred syndrome (PDS) gene in human thyroid tissues. *J Clin Endocrinol Metab* 85:2028–2033
  49. Kondo T, Nakamura N, Suzuki K, Murata S, Muramatsu A, Kawaoi A, Katoh R 2003 Expression of human pendrin in diseased thyroids. *J Histochem Cytochem* 51:167–171
  50. Porra V, Ferraro-Peyret C, Durand C, Selmi-Ruby S, Giroud H, Berger-Dutrieux N, Decaussin M, Peix JL, Bournaud C, Orgiazzi J, Borson-Chazot F, Dante R, Rousset B 2005 Silencing of the tumor suppressor gene SLC5A8 is associated with BRAF mutations in classical papillary thyroid carcinomas. *J Clin Endocrinol Metab* 90:3028–3035
  51. Wagner CA, Finberg KE, Stehberger PA, Lifton RP, Giebisch GH, Aronson PS, Geibel JP 2002 Regulation of the expression of the Cl<sup>-</sup>/anion exchanger pendrin in mouse kidney by acid-base status. *Kidney Int* 62:2109–2117
  52. Frische S, Kwon TH, Frokiaer J, Madsen K, Nielsen S 2003 Regulated expression of pendrin in rat kidney in response to chronic NH<sub>4</sub>Cl or NaHCO<sub>3</sub> loading. *Am J Physiol Renal Physiol* 284:584–593
  53. Petrovic S, Wang Z, Ma L, Soleimani M 2003 Regulation of the apical Cl<sup>-</sup>/HCO<sub>3</sub><sup>-</sup> exchanger, pendrin, in rat cortical collecting duct in metabolic acidosis. *Am J Physiol Renal Physiol* 284:103–112
  54. Quentin F, Chambrey R, Tringh-Tran-Tan MM, Fysekidis M, Cambillau M, Paillard M, Aronson PS, Eladari D 2004 The Cl<sup>-</sup>/HCO<sub>3</sub><sup>-</sup> exchanger, pendrin, of the rat kidney is regulated in response to chronic alterations in chloride balance. *Am J Physiol Renal Physiol* 287:1179–1188